Simultaneous description of low-lying positive and negative parity bands in heavy even-even nuclei

H. G. Ganev
Joint Institute for Nuclear Research, 141980 Dubna, Russia
(Received 17 February 2014; revised manuscript received 4 April 2014; published 12 May 2014)

The low-lying spectra including the first few excited positive and negative parity bands of some heavy even-even nuclei from the rare earth and actinide mass regions are investigated within the framework of the symplectic interacting vector boson model with the Sp(12,R) dynamical symmetry group. Symplectic dynamical symmetries allow the change of the number of excitation quanta or phonons building the collective states, providing for larger representation spaces and richer subalgebraic structures to incorporate more complex nuclear spectra. The theoretical predictions for the energy levels and the electromagnetic transitions between the collective states of the ground-state band and $K^{\pi}=0^{-}$ band are compared with experiment and some other collective models incorporating octupole and/or dipole degrees of freedom. The energy staggering, which is a sensitive indicator of the octupole correlations in even-even nuclei, is also calculated and compared with experiment. The results obtained for the energy levels, energy staggering, and transition strengths reveal the relevance of the dynamical symmetry used in the model to simultaneously describe both positive and negative parity low-lying collective bands.

DOI: 10.1103/PhysRevC.89.054311 PACS number(s): 21.10.Re, 21.60.Fw, 23.20.Lv, 27.60.+j

I. INTRODUCTION

It is well known [1,2] that in some mass regions several bands of negative parity are observed in the low-lying nuclear spectra in even-even nuclei, like the $K^{\pi}=0^{-}$, 1^{-}, and 2^{-} bands. The most well studied of them is the $K^{\pi}=0^{-}$ band, usually interpreted as an octupole vibrational band, connected to the ground-state band (GSB) by enhanced $E1$ transitions.

Negative parity states have been described within different approaches mainly by inclusion of octupole or/and dipole degrees of freedom. The bands of negative parity states are often associated with the reflection asymmetry in the intrinsic frame of reference. In the geometrical approach this is achieved by including of the $\alpha_{30}\equiv\beta_3$ deformation [3]. In the interacting boson model (IBM) [4] the description of negative states requires the introduction of f or/and p bosons with negative parity in addition to the standard s and d bosons ($spdf$-IBM) [5,6]. An alternative interpretation of the low-lying negative parity states has been provided in different cluster models [7,8] in which the dipole degrees of freedom are related with the relative motion of the clusters. Based on the Bohr Hamiltonian different critical-point symmetries (CPS) including axial quadrupole and octupole deformations have been proposed [9–12] extending the concept of CPS introduced for the description of positive parity states.

In this paper we present an algebraic approach, complementary to the $spdf$-IBM [5], for the unified description of the low-lying positive and negative parity bands in some even-even nuclei from the rare earth and actinide mass regions within the framework of the symplectic interacting vector boson model (IVBM) with Sp(12,R) dynamical symmetry group [13]. The present work is an extension of the approach proposed in Ref. [14] for the description of the ground-state band and the "octupole" ($K^{\pi}=0^{-}$) band, often treated as a single-ground-state alternating-parity band. In this way we investigate simultaneously the first few low-lying negative parity bands ($K^{\pi}=0^{-}$, 1^{-}, and 2^{-}) together with the first few positive parity (ground-state, β, and γ) bands. It is shown that the negative parity bands arise along with the positive bands without introducing any additional collective degrees of freedom. Additionally, we calculate the strengths of the intraband $E2$ transitions in both the GSB and $K^{\pi}=0^{-}$ band, as well as the interband $E1$ transitions connecting the states of these two bands. The energy staggering of the ground-state alternating band, which is a sensitive indicator of the octupole correlations in the even-even nuclei, is also calculated and compared with experiment.

II. THEORETICAL FRAMEWORK

A. Interacting vector boson model

It was suggested by Bargmann and Moshinsky [15,16] that two types of bosons are needed for the description of nuclear dynamics. It was shown there that the consideration of only a two-body system consisting of two different interacting vector particles will suffice to give a complete description of N three-dimensional oscillators with a quadrupole-quadrupole interaction. The latter can be considered as the underlying basis in the algebraic construction of the *phenomenological* IVBM [13].

The algebraic structure of the IVBM is realized in terms of creation and annihilation operators of two kinds of vector bosons $u_m^{\dagger}(\alpha)$, $u_m(\alpha)$ ($m=0,\pm 1$), which differ in an additional quantum number $\alpha=\pm 1/2$ (or $\alpha=p$ and n)—the projection of the T-spin (an analog to the F-spin of IBM-2 or the I-spin of the particle-hole IBM). All bilinear combinations of the creation and annihilation operators of the two vector bosons generate the boson representations of the noncompact symplectic group Sp(12,R):

$$F_M^L(\alpha,\beta)=\sum_{k,m}C_{1k1m}^{LM}u_k^{+}(\alpha)u_m^{+}(\beta), \qquad (1)$$

$$G_M^L(\alpha,\beta)=\sum_{k,m}C_{1k1m}^{LM}u_k(\alpha)u_m(\beta), \qquad (2)$$

$$A_M^L(\alpha,\beta)=\sum_{k,m}C_{1k1m}^{LM}u_k^{+}(\alpha)u_m(\beta), \qquad (3)$$

where C^{LM}_{1k1m}, which are the usual Clebsch-Gordan coefficients for $L = 0,1,2$ and $M = -L, -L+1, \ldots, L$, define the transformation properties of (1), (2), and (3) under rotations. The number preserving operators (3) generate the U(6) group, while by adding the pair creation (1) and annihilation (2) operators we generate the noncompact Sp(12,R) which is the dynamical group of the IVBM. Its irreducible representations are infinite dimensional. We also introduce the following notations for the two bosons: $u^\dagger_m(\alpha = 1/2) = p^\dagger_m$ and $u^\dagger_m(\alpha = -1/2) = n^\dagger_m$.

Symplectic dynamical symmetries allow the change of the number of bosons, elementary excitations, or phonons N, providing for richer subalgebraic structures and larger representation spaces to accommodate more structural effects. The dynamical symmetry group Sp(12,R) contains both compact and noncompact substructures, which are defined by different reduction chains.

B. Dynamical symmetry

We consider the following chain [13,14]:

$$\begin{array}{ccccccc} \mathrm{Sp}(12,R) \supset & \mathrm{U}(6) \supset & \mathrm{SU}(3) & \otimes & \mathrm{U}(2) & \supset \mathrm{SO}(3) \otimes & U(1), \\ & [N]_6 & (\lambda,\mu) & \Longleftrightarrow & (N,T) & K \quad L & T_0 \end{array} \tag{4}$$

where below the different subgroups the quantum numbers characterizing their irreducible representations are given. The generators of the different subgroups in Eq. (4) are expressed in terms of the number-preserving operators (3). The number operator

$$N = p^\dagger \cdot p + n^\dagger \cdot n = N_p + N_n \tag{5}$$

is the linear invariant of the U(6) as well as U(3) and U(2) algebras. The SU(3) algebra is generated by the components of the angular momentum operators

$$L_M = -\sqrt{2} \sum_\alpha A^1_M(\alpha,\alpha) \tag{6}$$

and Elliott's quadrupole operators

$$Q_M = \sqrt{6} \sum_\alpha A^2_M(\alpha,\alpha). \tag{7}$$

The T-spin operators

$$T_{+1} = -\frac{1}{\sqrt{2}} p^\dagger \cdot n, \tag{8}$$

$$T_{-1} = \frac{1}{\sqrt{2}} n^\dagger \cdot p, \tag{9}$$

$$T_0 = \frac{1}{2}(p^\dagger \cdot p - n^\dagger \cdot n), \tag{10}$$

together with the number operator (5) generate the U(2) algebra.

Within the symmetric irreducible representation $[N]_6$ of U(6) the groups SU(3) and U(2) are mutually complementary [17], i.e., the quantum numbers (λ,μ) are related with (N,T) in the following way: $N = \lambda + 2\mu$ and $T = \lambda/2$. Making use of the latter we can write the basis as

$$|[N]_6; (\lambda,\mu); K,L; T_0\rangle = |(N,T); K,L; T_0\rangle. \tag{11}$$

TABLE I. Classification of basis states.

N	T	$T_0 \cdots$	-3	-2	-1	0	1	2	3	$\cdots$
0	0					(0, 0)				
2	1				(2, 0)	(2, 0)	(2, 0)			
	0					(0, 1)				
4	2			(4, 0)	(4, 0)	(4, 0)	(4, 0)	(4, 0)		
	1				(2, 1)	(2, 1)	(2, 1)			
	0					(0, 2)				
6	3		(6, 0)	(6, 0)	(6, 0)	(6, 0)	(6, 0)	(6, 0)	(6, 0)	
	2			(4, 1)	(4, 1)	(4, 1)	(4, 1)	(4, 1)		
	1				(2, 2)	(2, 2)	(2, 2)			
	0					(0, 3)				
$\cdots$	$\cdots$	$\cdots$	$\cdots$	$\cdots$	$\cdots$	$\cdots$	$\cdots$	$\cdots$	$\cdots$	$\cdots$

The ground state of the system is

$$|0\rangle = |(N=0,T=0); K=0,L=0; T_0=0\rangle, \tag{12}$$

which is the vacuum state for the Sp(12,R) group.

The basis states associated with the even irreducible representation of the Sp(12,R) can be constructed by the application of powers of raising generators $F^L_M(\alpha,\beta)$ of the same group on the vacuum. Each raising operator will increase the number N of bosons by two. The resulting infinite set of basis states so obtained is denoted as in Eq. (11) and is shown in Table I. Each row (fixed N) of the table corresponds to a given U(6) irrep, whereas each cell represents the SU(3) irrep contained in the corresponding U(6) irrep. For fixed N, the possible values for the T-spin are $T = \frac{N}{2}, \frac{N}{2} - 1, \ldots, 0$ and are given in the column next to the respective value of N. Thus when N and T are fixed, $2T+1$ equivalent representations (λ,μ) of the group SU(3) arise. Each of them is labeled by the eigenvalues of the operator $T_0 : -T, -T+1, \ldots, T$, defining the columns of Table I. The values of the angular momentum contained in a certain SU(3) representation (λ,μ) are obtained by means of standard reduction rules for the chain SU(3) $\supset$ SO(3) [18]:

$$\begin{aligned} K &= \min(\lambda,\mu),\ \min(\lambda,\mu) - 2, \ldots, 0\,(1), \\ L &= \max(\lambda,\mu),\ \max(\lambda,\mu) - 2, \ldots, 0\,(1); \quad K = 0, \\ L &= K, K+1, \ldots, K + \max(\lambda,\mu); \quad K \neq 0. \end{aligned} \tag{13}$$

The multiplicity index K appearing in this reduction is related to the projection of L in the body fixed frame and is used with the parity (π) to label the different bands (K^π) in the energy spectra of the nuclei.

C. The Hamiltonian

We use the following Hamiltonian [14]:

$$H = aN + bN^2 + \alpha_3 T^2 + \beta_3 L^2 + \alpha_1 T_0^2, \tag{14}$$

expressed in terms of the first- and second-order invariant operators of the different subgroups in the chain (4). It is obviously diagonal in the basis (11) and its eigenvalues are just the energies of the nuclear system

$$\begin{aligned} E(N,L,T,T_0) = {} & aN + bN^2 + \alpha_3 T(T+1) \\ & + \beta_3 L(L+1) + \alpha_1 T_0^2. \end{aligned} \tag{15}$$

The energy of the ground state (12) of the system is obviously 0.

III. APPLICATION

In our application, the most important point is the identification of the experimentally observed states with a certain subset of the basis states (11). In this regard, the following two points are of importance. First, as we noted, the irreducible representations of Sp(12,R) are infinite dimensional. Then we require the truncation of the model space to a finite-dimensional subspace of physically meaningful basis states revealing the collective properties of states described. It turns out that such an appropriate set of states is given by the so-called "stretched states" [19], which represent dominant SU(3) multiplets in the low-lying collective states [19]. In the present application we use the following type of stretched states defined as the SU(3) states of the type $(\lambda,\mu) = (\lambda_0,\mu_0 + k)$, where $k = 0,2,4,\ldots$. In the symplectic IVBM the change of the number k, which is related in the applications to the angular momentum L of the states, gives rise to the collective bands.

The second point concerns the parity of the state. We assume that the one type of the two vector bosons, say the p-boson, transforms under space reflections as a pseudovector, while the other – the n-boson – transforms as a vector. The latter assumes that the creation operators of the two vector bosons, $p_m^\dagger$ and $n_m^\dagger$, can be considered as acting separately in the two adjacent major oscillator shells of opposite parity, creating in this way two different elementary excitations ("Elliott quarks," see Ref. [20]) with opposite parity from which the collective states are built out. Therefore, we define the

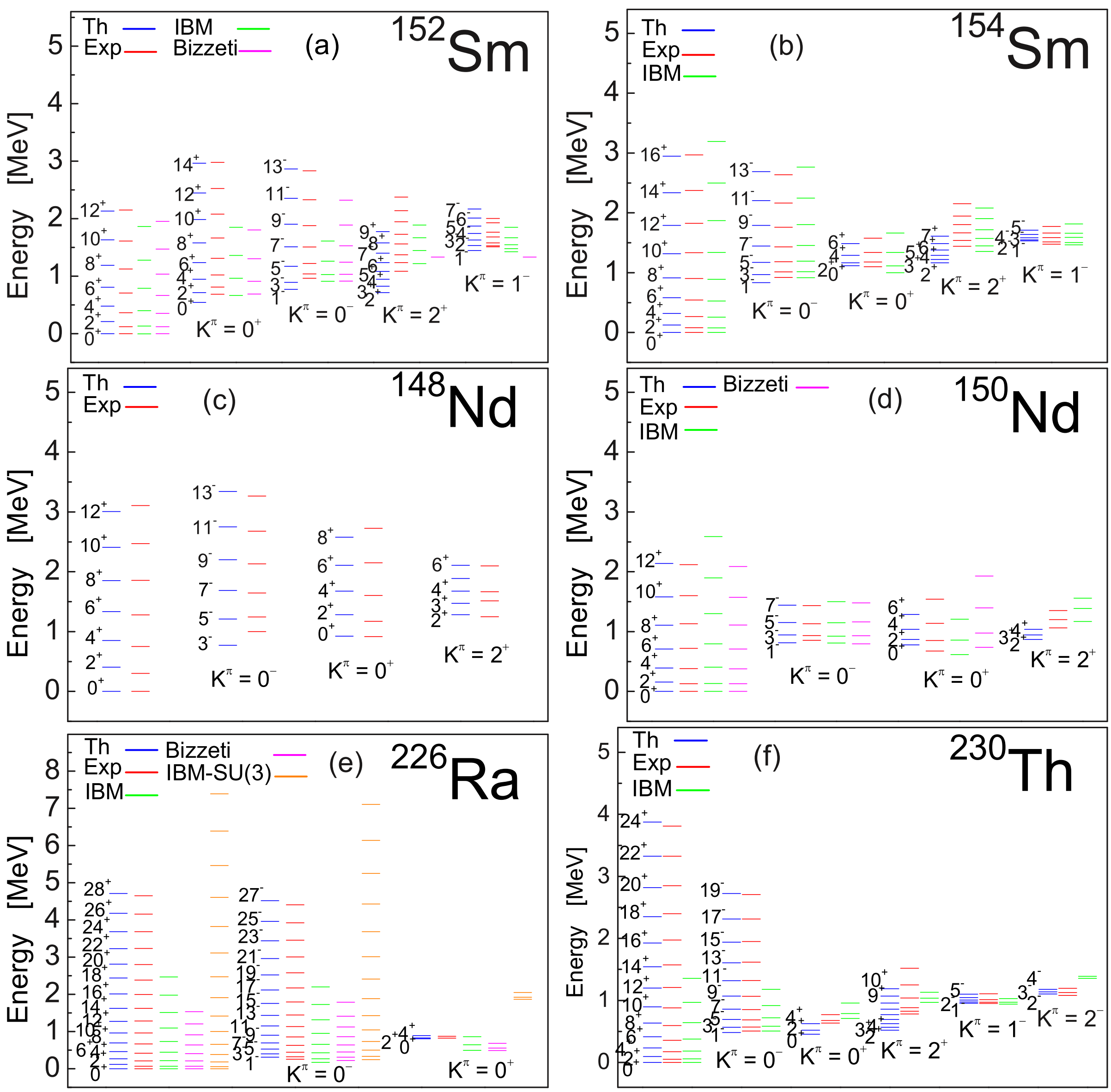

FIG. 1. (Color online) Comparison of the theoretical energies for the low-lying positive and negative parity bands in ^{152}Sm, ^{154}Sm, ^{148}Nd, ^{150}Nd, ^{226}Ra, and ^{230}Th with experiment and some other collective models incorporating octupole or/and dipole degrees of freedom.

parity of the considered collective state as $\pi = (-1)^{N_n}$, which generalizes our previous definition of the parity $\pi = (-1)^T$ given in Ref. [14]. This allows us to describe both positive and negative parity states in the IVBM on the same footing without introducing of any additional collective degrees of freedom.

In this way for example, the states of the ground-state band are mapped onto the SU(3) multiplets $(0,L)$ ($T = 0$, $T_0 = 0$) with $L = 0,2,4,\ldots$, whereas those of the $K^\pi = 0^-$ band are mapped onto the SU(3) multiplets $(2,L)$ ($T = 1$, $T_0 = 1$) with $L = 1,3,5,\ldots$. The latter mapping slightly differs from that used in Ref. [14] with ($T = 1$, $T_0 = 0$) because of the parity definition. We note that although the set of SU(3) states used in Ref. [14] and in the present approach is identical, in order to take into account proper the parity of the collective states, we need the appropriate values of both T and T_0. Note that the SU(3) degeneracy within a given U(6) irrep is lifted by its mutually complimentary group U(2). The same type of the stretched states $(\lambda,\mu) = (\lambda_0,\mu_0 + k)$ are also used for other bands under consideration.

A. Energy spectra

We consider the first few excited low-lying positive (ground-state, β, γ) and negative ($K^\pi = 0^-$, 1^-, 2^-) parity bands of some nuclei from the rare earth and light actinide regions for which there is enough experimental data on $E1$ and $E2$ transitions.

In Fig. 1 we compare our theoretical predictions for the energies of the first-excited positive and negative parity bands observed in ^{152}Sm, ^{154}Sm, ^{148}Nd, ^{150}Nd, ^{226}Ra, and ^{230}Th with experiment [1] and the results obtained by the diagonalization of the $spdf$-IBM Hamiltonian [21] (^{152}Sm, ^{154}Sm), [22] (^{150}Nd), [23] (^{226}Ra, ^{230}Th). For the ^{152}Sm, ^{150}Nd, and ^{226}Ra isotopes, the predictions of the CPS approach [10,11] in which the octupole degrees of freedom are included together with the quadrupole degrees of freedom are also shown. In the case of ^{226}Ra the results of the pure SU(3) dynamical limit of the $spdf$-IBM are shown as well. The calculations in the SU(3) limit of $spdf$-IBM are performed using the Hamiltonian and matrix elements given in Ref. [24]. The values of the model parameters obtained in the fitting procedure are given in Table II.

The ^{152}Sm and ^{150}Nd isotopes in the positive parity part (GSB and β band) of the spectrum are considered as examples of the X(5) critical-point symmetry [25]. The nucleus ^{226}Ra is considered in the literature as possessing stable octupole shape. ^{230}Th is considered as an octupole soft nucleus in

TABLE II. The values of the model parameters (in MeV).

Nucleus	a	b	α_3	β_3	α_1
^{152}Sm	0.02792	−0.00176	0.10948	0.01551	0.46287
^{154}Sm	0.01476	−0.00153	0.06864	0.01486	0.63245
^{148}Nd	0.09149	−0.00155	0.09725	0.01094	−0.18550
^{150}Nd	0.01572	−0.00413	0.95750	0.02656	−1.1522
^{226}Ra	0.01581	−0.00278	0.12640	0.01600	0.00523
^{230}Th	0.01248	−0.00204	0.15437	0.01331	0.13035

a recent constrained self-consistent relativistic mean-field calculation [26].

One sees that the IVBM describes reasonably well the structure of low-lying excited states of the first few bands of positive and negative parity up to high angular momenta for the all nuclei under consideration. Note that, in the case of ^{226}Ra, the experimental data show large deviations from the rotational $L(L+1)$ rule [SU(3) limit of the $spdf$-IBM] for both the ground state and $K^\pi = 0^-$ bands despite the fact that $R_{4/2} = 3.13$.

B. Energy staggering

A convenient measure for deviation from the pure rotational behavior is the signature-splitting index $S(L)$ [27]:

$$S(L) = \frac{[E_{L+1} - E_L] - [E_L - E_{L-1}]}{E_{2_1^+}}, \qquad (16)$$

which vanishes for

$$E(L) = E_0 + AL(L+1), \qquad (17)$$

but not for

$$E(L) = E_0 + AL(L+1) + B[L(L+1)]^2. \qquad (18)$$

Another quantity also used in practice is [28]

$$\Delta E_{\gamma,1}(L) = \tfrac{1}{16}[6\Delta E(L) - 4\Delta E(L-1) - 4\Delta E(L+1) + \Delta E(L+2) + \Delta E(L-2)], \qquad (19)$$

where $\Delta E(L) = E(L) - E(L-1)$. The staggering function (19), in contrast to Eq. (16), vanishes for (18) and hence it represents a more sensitive measure for the deviation of the nuclear dynamics from that of pure rotational motion. We recall that the SU(3) limit of the $spdf$-IBM predicts [28] a constant behavior for the staggering function (19), thus being unable to describe the latter.

In the present work we consider the odd-even staggering between the states of the GSB and $K^\pi = 0^-$ band. The mapping of the experimentally observed states of the two bands under considerations onto the basis states of Table I ("stretched approximation") establishes a relationship between the quantum numbers N and L. As a result, the energies of the GSB can be expressed in the form [14]

$$E(L) = \beta L(L+1) + \gamma L, \qquad (20)$$

whereas those of the $K^\pi = 0^-$ band can be expressed as

$$E(L) = \beta L(L+1) + (\gamma + \eta)L + \xi. \qquad (21)$$

The relation between the new set of parameters entering Eqs. (20) and (21) and that in Eq. (15) is given in Ref. [14]. From the expressions (20) and (21), one can see that the energies of the GSB and $K^\pi = 0^-$ band consist of rotational $L(L+1)$ and vibrational L terms. The rotational interaction is with equal strength β in both bands.

The calculated and experimental staggering patterns for all considered nuclei are illustrated in Fig. 2. As can be seen, the IVBM describes well the energy staggering, including the "beat patterns" (^{226}Ra). The first beat pattern appears at the

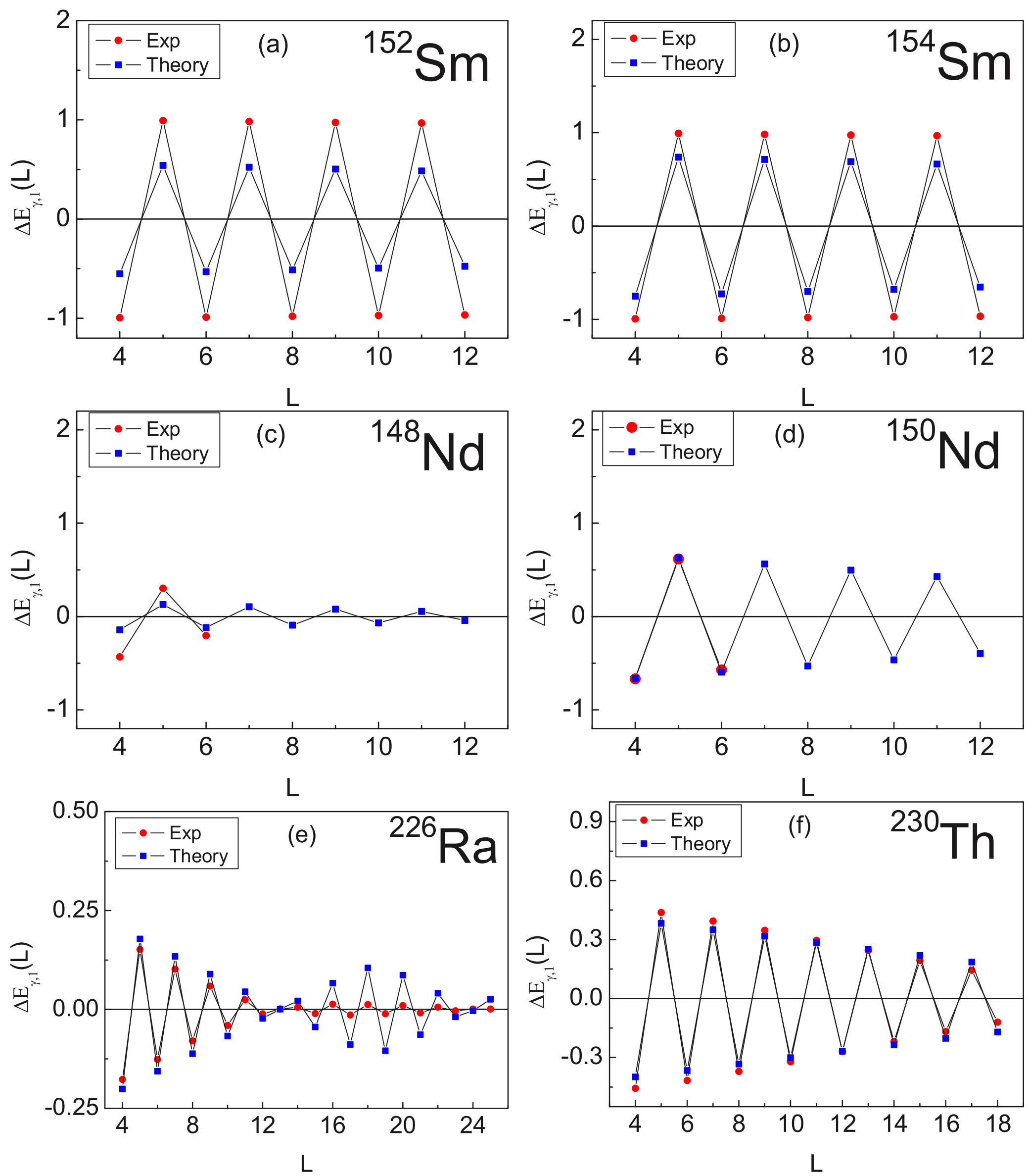

FIG. 2. (Color online) Theoretical and experimental staggering function $\Delta E_{\gamma,1}(L)$ [Eq. (19)] in ^{152}Sm, ^{154}Sm, ^{148}Nd, ^{150}Nd, ^{226}Ra, and ^{230}Th.

point where the two bands are crossing. In order to be able to describe the second beat pattern we assume that the states of the yrast band with high angular momentum ($L \geqslant 20$) are members of the first-excited β band. The correct reproduction of the experimental energy staggering, including the beat patterns, is due to the mixing of different collective modes

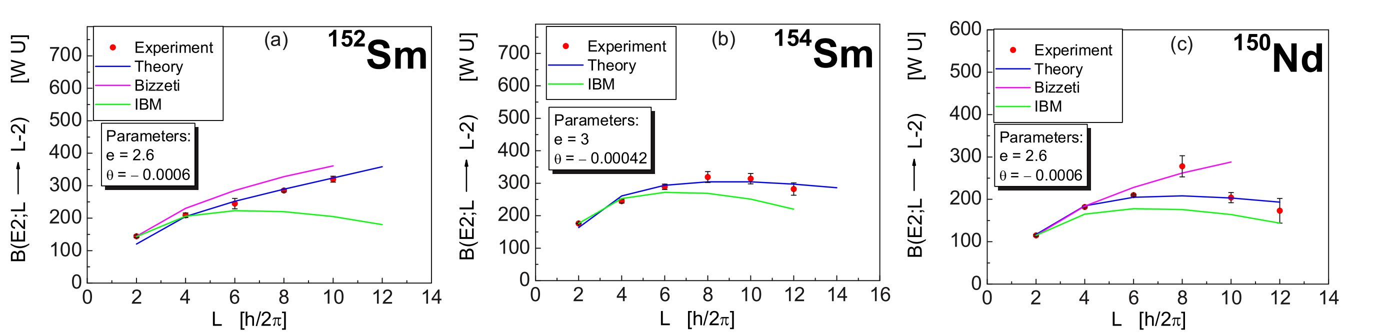

FIG. 3. (Color online) Comparison of theoretical and experimental values for the transition probabilities of the intraband $E2$ transitions in the ground-state band in ^{152}Sm, ^{154}Sm, and ^{150}Nd. For comparison, the theoretical predictions of some other collective models are also shown.

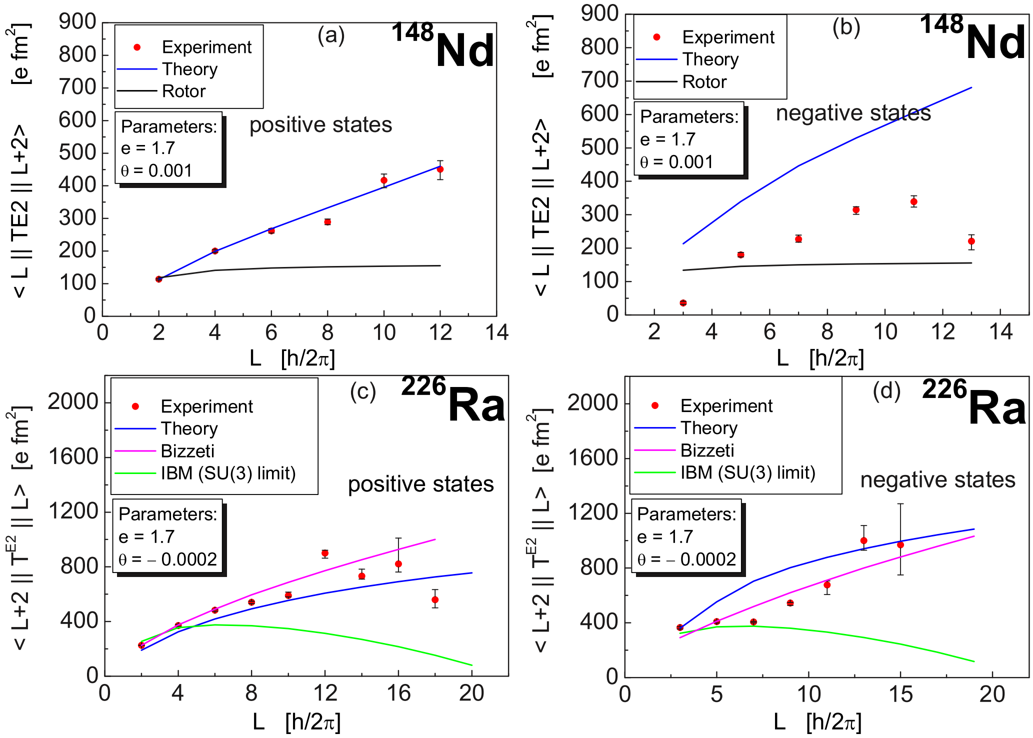

FIG. 4. (Color online) Comparison of theoretical and experimental values for the matrix elements of the intraband $E2$ transitions in the ground-state band and $K^\pi = 0^-$ band in ^{148}Nd and ^{226}Ra. For comparison, the theoretical predictions of some other collective models are also shown.

[see Eqs. (20) and (21)] within the framework of the symplectic IVBM. The mixing of the two bands under consideration is caused by the L-dependent interaction term ηL in Eq. (21).

C. Transition probabilities

It is well known that the transition probabilities are a more sensitive test for each model. Negative parity states of the $K^\pi = 0^-$ band are characterized by the enhanced $E1$ transition strengths to the GSB. In the present work we consider only the $B(E1)$ and $B(E2)$ transition probabilities concerning the ground-state and $K^\pi = 0^-$ bands.

The transition probabilities between the collective states attributed to the basis states of the Hamiltonian are by definition the square of the SO(3) reduced matrix elements of the transition operators:

$$B(E\lambda; L_i \to L_f) = \frac{1}{2L_i + 1} |\langle f || T^{E\lambda} || i \rangle|^2. \tag{22}$$

The general approach for calculating the transition probabilities along the considered dynamical symmetry is given in Ref. [29], where the $B(E2)$ transition probabilities between the states of the GSB were calculated. Similarly, in the present work we calculate the strengths of the intraband $E2$ transitions in both the GSB and $K^\pi = 0^-$ band, as well as the interband $E1$ transitions connecting the states of these two bands. In our calculations, we use the following operators:

$$T^{E2} = e\Big[A^{[1,-1]_6 \;\; 20}_{(1,1)[0]_2 \;\; 00} + \theta\Big([F \times F]^{[4]_6 \;\; 20}_{(0,2)[0]_2 \;\; 00} + [G \times G]^{[-4]_6 \;\; 20}_{(2,0)[0]_2 \;\; 00}\Big)\Big], \tag{23}$$

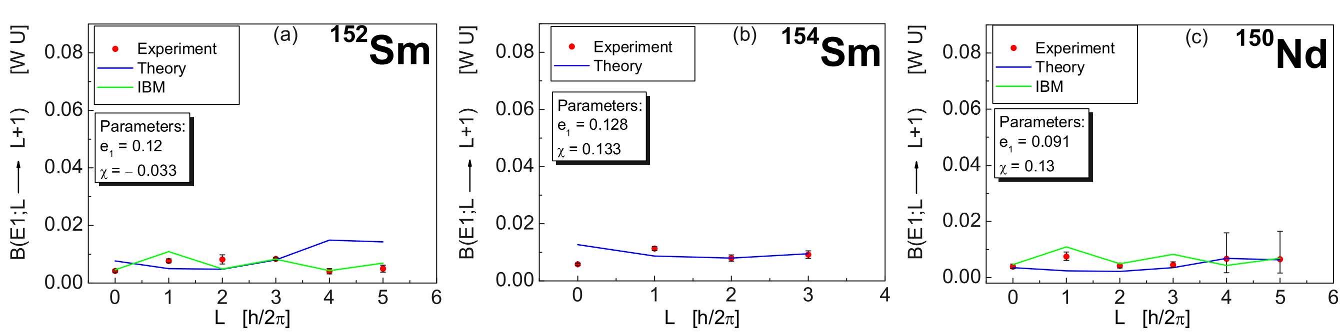

FIG. 5. (Color online) Comparison of theoretical and experimental values for the transition probabilities of the interband $E1$ transitions between the states of the GSB and $K^\pi = 0^-$ band in ^{152}Sm, ^{154}Sm, and ^{150}Nd. For comparison, the theoretical predictions of the IBM are also shown.

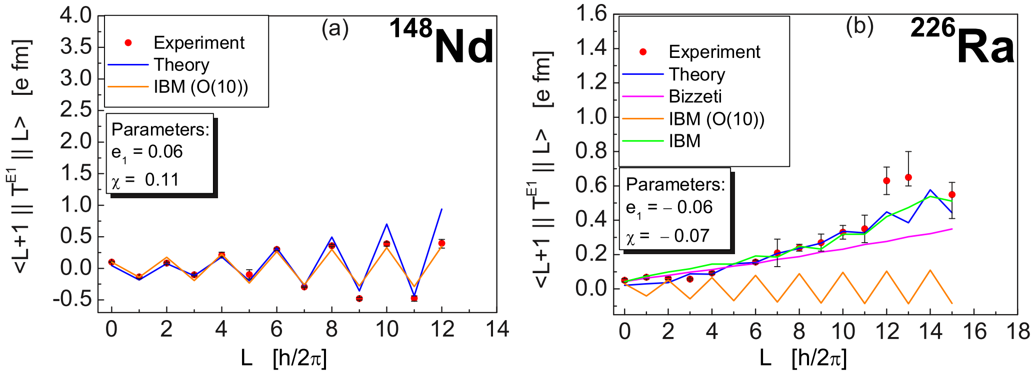

FIG. 6. (Color online) Comparison of theoretical and experimental values for the matrix elements of the interband $E1$ transitions between the states of the GSB and $K^\pi = 0^-$ band in ^{148}Nd and ^{226}Ra. For comparison, the theoretical predictions of some other collective models are also shown.

and

$$\begin{aligned} T^{E1} =& e_1\big[A^{[1,-1]_6}_{(1,1)[2]_2}{}^{10}_{1-1} + \chi\big([F\times F]^{[4]_6}_{(2,1)[2]_2}{}^{10}_{11} \\ &+ [G\times G]^{[-4]_6}_{(1,2)[-2]_2}{}^{10}_{1-1}\big)\big], \end{aligned} \tag{24}$$

as transition operators for the $E2$ and $E1$ transitions, respectively. In Eqs. (23) and (24) explicit tensor properties with respect to the reduction chain (4) are written. For more details concerning the calculations we refer the reader to Ref. [29].

In Fig. 3 we compare our theoretical results for the transition probabilities of the intraband $E2$ transitions in the ground-state band for the three isotopes ^{152}Sm, ^{154}Sm, and ^{150}Nd. Figure 4 compares with experiment the theoretical matrix elements of the intraband $E2$ transitions in both the ground-state band and the $K^\pi = 0^-$ band for ^{148}Nd and ^{226}Ra nuclei. For comparison, the theoretical predictions of some other collective models are also shown. We see that IVBM describes reasonably well the general trend of the experimental data. An enhancement of the theoretical $E2$ matrix elements in the $K^\pi = 0^-$ band compared to the GSB values is obtained. Such an enhancement was experimentally observed in ^{144}Ba [30].

In Figs. 5 and 6 the calculated transition strengths (matrix elements or transition probabilities) for the $E1$ transitions connecting the states of the GSB and $K^\pi = 0^-$ band are compared with experiment [1,31] (^{226}Ra), [32] (^{148}Nd), and the predictions of some other collective models incorporating octupole or/and dipole degrees of freedom.

An interesting zigzagging behavior of the matrix elements of the $E1$ transitions is observed in the case of ^{148}Nd. Such a staggering behavior with correct phases is obtained in the framework of the *spdf*-IBM if the O(10) generator is used as a transition operator. An equivalent picture is obtained if the O(4) generator is used as a transitional operator instead of the O(10) generator. From Fig. 6 one sees that IVBM is also able to describe such staggering behavior.

IV. CONCLUSIONS

In the present work the low-lying spectra including the first few excited positive and negative parity bands of some heavy even-even nuclei from the rare earth and actinide mass regions, namely ^{152}Sm, ^{154}Sm, ^{148}Nd, ^{150}Nd, ^{226}Ra, and ^{230}Th, are investigated within the framework of the symplectic interacting vector boson model with the Sp(12,R) dynamical symmetry group. Symplectic dynamical symmetries allow us to change the number of excitation quanta or phonons that build the collective states, providing for larger representation spaces and richer subalgebraic structures to incorporate more complex nuclear spectra. The theoretical predictions for the energy levels, energy staggering and transition strengths between the collective states are compared with experiment and some other collective models incorporating octupole or/and dipole degrees of freedom. The IVBM describes well the experimental data, including some structural effects observed in the nuclear spectra such as the beat patterns (^{226}Ra) in the energy staggering. The results obtained for the energy levels, the energy staggering and the transition strengths in the considered nuclei prove the correct mapping of the basis states to the experimentally observed states and reveal the relevance of the dynamical symmetry used in the IVBM for the simultaneous description of the lowlying positive and negative parity bands.

[1] National Nuclear Data Center, http://www.nndc.bnl.gov/
[2] P. A. Butler and W. Nazarewicz, Rev. Mod. Phys. **68**, 349 (1996).
[3] A. Bohr and B. R. Mottelson, Nucl. Phys. **4**, 529 (1957).
[4] F. Iachello and A. Arima, *The Interacting Boson Model* (Cambridge University Press, Cambridge, 1987).
[5] C. S. Han *et al.*, Phys. Lett. B **163**, 295 (1985).
[6] J. Engel and F. Iachello, Phys. Rev. Lett. **54**, 1126 (1985); Nucl. Phys. A **472**, 61 (1987).
[7] F. Iachello and A. D. Jackson, Phys. Lett. B **108**, 151 (1982); F. Iachello, Nucl. Phys. A **396**, 233c (1983); H. Daley and F. Iachello, Phys. Lett. B **131**, 281 (1983); H. J. Daley and F. Iachello, Ann. Phys. (Amsterdam, Neth.) **167**, 73 (1986).
[8] T. M. Shneidman *et al.*, Phys. Lett. B **526**, 322 (2002).

[9] P. G. Bizzeti and A. M. Bizzeti-Sona, Phys. Rev. C **70**, 064319 (2004).
[10] P. G. Bizzeti and A. M. Bizzeti-Sona, Phys. Rev. C **77**, 024320 (2008).
[11] P. G. Bizzeti and A. M. Bizzeti-Sona, Phys. Rev. C **81**, 034320 (2010).
[12] D. Bonatsos, D. Lenis, N. Minkov, D. Petrellis, and P. Yotov, Phys. Rev. C **71**, 064309 (2005); D. Lenis and D. Bonatsos, Phys. Lett. B **633**, 474 (2006).
[13] A. Georgieva, P. Raychev, and R. Roussev, J. Phys. G **8**, 1377 (1982).
[14] H. Ganev, V. P. Garistov, and A. I. Georgieva, Phys. Rev. C **69**, 014305 (2004).
[15] V. Bargmann and M. Moshynsky, Nucl. Phys. **18**, 697 (1960).
[16] V. Bargmann and M. Moshynsky, Nucl. Phys. **23**, 177 (1961).
[17] M. Moshinsky and C. Quesne, J. Math. Phys. **11**, 1631 (1970).
[18] J. P. Elliott, Proc. Roy. Soc. A **245**, 128 (1958); **245**, 562 (1958).
[19] D. J. Rowe, Rep. Prog. Phys. **48**, 1419 (1985).
[20] H. J. Lipkin, Nucl. Phys. A **350**, 16 (1980).
[21] M. Babilon, N. V. Zamfir, D. Kusnezov, E. A. McCutchan, and A. Zilges, Phys. Rev. C **72**, 064302 (2005).
[22] M. Elvers *et al.*, Phys. Rev. C **84**, 054323 (2011).
[23] N. V. Zamfir and D. Kusnezov, Phys. Rev. C **63**, 054306 (2001).
[24] H. Y. Ji *et al.*, Nucl. Phys. A **658**, 197 (1999); G. L. Long, T. Y. Shen, H. Y. Ji, and E. G. Zhao, Phys. Rev. C **57**, 2301 (1998).
[25] R. F. Casten and N. V. Zamfir, Phys. Rev. Lett. **87**, 052503 (2001).
[26] K. Nomura, D. Vretenar, and B. N. Lu, Phys. Rev. C **88**, 021303(R) (2013).
[27] N. V. Zamfir, P. von Brentano, and R. F. Casten, Phys. Rev. C **49**, R605 (1994).
[28] D. Bonatsos, C. Daskaloyannis, S. B. Drenska, N. Karoussos, N. Minkov, P. P. Raychev, and R. P. Roussev, Phys. Rev. C **62**, 024301 (2000).
[29] H. G. Ganev and A. I. Georgieva, Phys. Rev. C **76**, 054322 (2007).
[30] T. M. Shneidman *et al.*, Eur. Phys. J. A **25**, 387 (2005).
[31] H. J. Wollersheim *et al.*, Nucl. Phys. A **556**, 261 (1993).
[32] R. W. Ibbotson *et al.*, Nucl. Phys. A **619**, 213 (1997).